RSC Advances

PAPER

View Article Online
View Journal | View Issue

Cite this: *RSC Adv.*, 2023, **13**, 30190

Two polysaccharides from *Rehmannia glutinosa*: isolation, structural characterization, and hypoglycemic activities†

Huien Chen,‡[abc] Xinyu Liu,‡[abc] Meixia Xie,‡[abc] Xiaoting Zhong,[abc] Chunyan Yan,*[a] Minghua Xian *[abc] and Shumei Wang*[abc]

Rehmannia glutinosa (RG) as a Chinese herbal medicine can be used both in medicine and food. As the main component of RG, the polysaccharides have a hypoglycemic effect, however, the hypoglycemic activity of RG homopolysaccharides remains unknown. We isolated and purified two polysaccharides, RGP70-1-1 and RGP70-1-2 (4.9 kDa and 2.8 kDa) from RG. The structural characteristics, including monosaccharide composition, linkage, and configuration were analyzed by FT-IR, HPLC, GC-MS, NMR spectroscopy, Congo test, and SEM. RGP70-1-1 and RGP70-1-2 consist of four monosaccharides (glucose, mannose, arabinose, and galactose). RGP70-1-1 contains 14 connection modes, with the linkages including L-Ara*f*-(1→, →3)-L-Ara*f*-(1→, →5)-L-Ara*f*-(1→, →3,5)-L-Ara*f*-(1→, →2,5)-L-Ara*f*-(1→, D-Man*p*-(1→, →2)-D-Man*p*-(1→, →4)-D-Man*p*-(1→, D-Gal*p*-(1→, →4)-D-Gal*p*-(1→, →4,6)-D-Gal*p*-(1→, →6)-D-Glc*p*-(1→, →4,6)-D-Glc*p*-(1→, →3,6)-D-Glc*p*-(1→. The linkages of RGP70-1-2 is including →5)-L-Ara*f*-(1→, →3,5)-L-Ara*f*-(1→, →4)-D-Man*p*-(1→, →3,6)-D-Man*p*-(1→, D-Gal*p*-(1→, →6)-D-Gal*p*-(1→, D-Glc*p*-(1→, →6)-D-Glc*p*-(1→, →4,6)-D-Glc*p*-(1→. Furthermore, RGP70-1-1 and RGP70-1-2 can inhibit α-glucosidase and α-amylase. RGP70-1-1 stimulated GLP-1 secretion in STC-1 cells and was related to the up-regulation of PI3K and p-AKT protein expression. The findings revealed a natural product with potential hypoglycemic activity, which may be used as a GLP-1 secretagogue and a beneficial functional food ingredient for T2D.

Received 20th August 2023
Accepted 24th September 2023

DOI: 10.1039/d3ra05677e

rsc.li/rsc-advances

1 Introduction

In 2021, the worldwide morbidity of diabetes among those aged 20 to 79 was estimated at 536.6 million. The number of people with diabetes is estimated to increase in 2045.[1] Diabetes has gradually become a severe social health problem worldwide, a metabolic disorder with symptoms of hyperglycemia due to insulin resistance and secretion abnormalities.[2] Long-term hyperglycemia will increase cardiovascular and cerebrovascular incidence rates, and may cause eye diseases and kidney function damage.[3] Therefore, it is significant to develop the prevention and treatment of type 2 diabetes (T2D).[4] Glucagon-like peptide-1 (GLP-1) secreted by intestinal L cells can control postprandial blood sugar by raising insulin and inhibiting glucagon secretion without causing hypoglycemia.[5] Additionally, GLP-1 inhibits gastric emptying and food intake and limits weight gain.[6] Thus, it has become a significant pharmaceutical target for discovering new drugs to treat T2D. Because dipeptidyl peptidase 4 (DPP-4) readily degrades GLP-1 *in vivo*, the plasma half-life of GLP-1 is less than 2 minutes, and it must be continuously administered intravenously to produce the curative effect, dramatically limiting the clinical application of GLP-1. Both GLP-1 analogues and DPP-4 inhibitors were developed to maintain the activity of GLP-1. However, both drugs have apparent disadvantages, for example, liraglutide and sigliptin will increase the risk of acute pancreatitis.[7] Therefore, it is imperative to find drugs with low toxicity and few side effects that can promote GLP-1 secretion in diabetic patients.

Rehmannia glutinosa (RG) is the dry root tuber of the plant *Rehmannia glutinosa* (Gaertn.) DC,[8] which can be fried, boiled, or soaked in wine in the diet book. RG is widely used in functional foods, traditional Chinese medicine prescriptions, and daily diets.[8] It has the functions of hypoglycemic, antioxidant,

[a]*Guangdong Pharmaceutical University, Guangzhou 510006, China. E-mail: gdpuwsm@126.com; xmh360@163.com*

[b]*Key Laboratory of Digital Quality Evaluation of Chinese Materia Medica of State Administration of TCM, Guangdong Pharmaceutical University, Guangzhou 510006, China*

[c]*Engineering & Technology Research Center for Chinese Materia Medica Quality of the Universities of Guangdong Province, Guangdong Pharmaceutical University, Guangzhou 510006, China*

† Electronic supplementary information (ESI) available: Fig. S1: ^{1}H-NMR (A), ^{13}C-NMR (B), ^{1}H–^{1}H COSY (C), HSQC (D) and HMBC (E) spectra of RGP70-1-2; Table S1: the chromatographic conditions of HPLC; Table S2: the program of HPLC gradient elution; Table S3: infrared spectral characteristic absorption peaks of RGP70-1-1 and RGP70-1-2; Table S4: the results of methylation analysis of RGP70-1-1; Table S5: the results of methylation analysis of RGP70-1-2. See DOI: https://doi.org/10.1039/d3ra05677e

‡ These authors contributed equally to this work.

hypolipidemic, and regulating immunity.[9–11] According to statistics, RG is widely used to formulate auxiliary hypoglycemic health foods.[12] Natural polysaccharides are widely recognized as safe and effective hypoglycemic agents with low toxicity and good pharmacological activity.[13] Polysaccharide, as the main component of RG, has a hypoglycemic effect.[14] At present, there have been some reports on the primary structure of RG polysaccharides (RGPs), but the hypoglycemic activity of RGPs is limited to RG water extract, oligosaccharide, and crude polysaccharide.[9,14] The relationship between RGPs and GLP-1 has yet to be clarified. Therefore, it is necessary to extract, isolate, and identify the monosaccharide from RG and clarify the components that play a fundamental hypoglycemic role in RG crude polysaccharide.

In this paper, two polysaccharides were isolated and purified from RG, and their structural characteristics were analyzed by HPLC, FT-IR, GC-MS, NMR spectroscopy, the Congo test, and SEM. In addition, the hypoglycemic ability of purified polysaccharides was explored through different *in vitro* enzyme activity experiments and cell experiments, and the role of RGP70-1-1 in promoting the excretion of GLP-1 from STC-1 was obtained through the detection of biochemical indicators. These findings indicate that RGP70-1-1 may have a hypoglycemic effect and potentially develop into a new hypoglycemic drug or health food. It may help develop novel medications for the treatment of T2D and improve the utilization rate of *Rehmannia glutinosa*.

2 Materials and methods

2.1. Materials

Rehmannia glutinosa Libosch was collected in Jiaozuo, Henan, China and purchased from Guangzhou Zhixin Chinese Herbal Pieces Co., Ltd (Guangzhou, China).

2.2. Extraction of crude RGPs

Through the processes of hot water extraction and ethanol precipitation, we obtained the crude polysaccharide of RG. The following were the experimental conditions: solid–liquid ratio of 1 : 10 (m/v), heat it to 85 °C, extract it 3 hours, extract it for three times, combine the extraction solution, and then further alkali extract the RG residue. We filtered, combined, and precipitated the extract with 85% ethanol. Moreover, it is stirred evenly until the ethanol concentration of the solution reaches 50%. After standing for 48 hours, the supernatant is concentrated, and 90% ethanol is then added to the concentrated solution until the solution's ethanol concentration reaches 70%. After standing for 48 hours, the precipitate obtained is the crude polysaccharide, named RGP70.

2.3. Isolation and purification of RGP70-1-1 and RGP70-1-2

The crude polysaccharide was soluble in H_2O and deproteinized by the Sevag method.[15] AB-8 macroporous adsorption resin was used to decolorize RGP70. After deproteinization and depigmentation, the polysaccharides solution (20 mg mL^{-1}) was isolated on a DEAE Cellulose-52 (specification Ø 2.5 × 45 cm, GE Healthcare), and eluted by various concentrations of NaCl (0, 0.05, 0.1 M) at a flow rate of 2.0 mL min^{-1}. The main elution part was obtained at 490 nm by the phenol-sulfuric acid method, and the polysaccharide-containing portions (RG70-1) were freeze-dried. After further elution and purification by the Sephacryl S-100 chromatography column (GE Healthcare) and purity verification by HPGPC, the polysaccharides with uniform molecular weight distribution were obtained RGP70-1-1 and RGP70-1-2.

2.4. Homogeneity verification and molecular weight determination

2.4.1. Specific rotation analysis. RGP70-1-1 and RGP70-1-2 were prepared into 60 mg mL^{-1} polysaccharide solutions, respectively. Ethanol was mixed with the solution until the final concentrations were 70% and 90% to obtain two precipitates, named precipitation I and II. Precipitates were freeze-dried and then reconstituted in water to gain a 1 mg mL^{-1} solution. The optical rotation was measured with an AUTOPOL 1 polarimeter (Rudolph Research Analytical, USA).

2.4.2. High-performance gel permeation chromatography (HPGPC). The uniformity of RGP70-1-1 and RGP70-1-2 was measured by HPGPC using a Waters 2414 refractive index detector and two Ultrahydrogel 1000 and Ultrahydrogel 500 columns connected in series. The mobile phase was 0.02 M KH_2PO_4 at a flow rate of 0.8 mL min^{-1}.

2.4.3. Matrix-assisted laser desorption ionization time-of-flight mass spectrometry (MALDI-TOF-MS). The molecular weights of the polysaccharides were analyzed by MALDI-TOF-MS. Detection conditions: reflection, linear scanning mode; the ionization method is a positive ion MALDI source; 2,5-Dihydroxybenzoic acid (DHB) serves as the substrate.

2.5. Structural characterization of RGP70-1-1 and RGP70-1-2

2.5.1. Monosaccharide composition. Aliquots of the polysaccharide fractions (5.0 mg) were hydrolyzed with 2 M TFA (Shanghai Aladdin Biochemical Technology) at 120 °C for 5 h, with stirring while heating. Then the sample was transferred to a 50 mL round-bottom flask, 6 mL of methanol was added to reduce pressure and concentrated to dry. Repeat this step at least three times, until the residual TFA is removed.

The polysaccharide sample was dissolved with 1 mL deionized water, then 200 μL of it was dissolved in the 5 mL sealed reaction tube. The same volume of 0.3 M NaOH and 0.5 M PMP (Shanghai Aladdin Biochemical Technology) methanol solution were added respectively, and reacted at 70 °C for 0.5 h. After the solution was cooled, a 0.3 M HCl solution of 212 μL was added. After neutralization, it was diluted with 100 μL deionized water before being extracted three times with 1 mL chloroform. The supernatant was used for HPLC analysis. The HPLC analysis was carried out on an Agilent 1260 system. The chromatographic conditions of HPLC are shown in Tables S1 and S2.† The mixed monosaccharide standard (mannose, galactose, glucose, glucuronic acid, rhamnose, arabinose, fucose, xylose and galacturonic acid (Shanghai Aladdin Biochemical Technology)) was subjected to the PMP derivatization reaction according to the same procedure.[16]

2.5.2. FT-IR spectroscopy analyses. The polysaccharides were mixed with the potassium bromide powder (spectrographic-grade) and then compressed into tablets. The Tensor-27 FT-IR spectrometer (FT/IR-100, PerkinEImer, USA) was used for detection in 4000–400 cm^{-1}.[17]

2.5.3. D/L configuration analysis. RGP70-1-1 and RGP70-1-2 were hydrolyzed according to method "2.5.1". After the hydrolysis product was dried, the sugar residue derivative reaction was carried out. The hydrolysate was dissolved in 1 mL pyridine, 2.5 mg L-cysteine methyl ester hydrochloride was added to it in water bath at 60 °C for 1 h, then 5 μL *o*-phenylisothioisocyanate was added, and then it was reacted in 60 °C water bath for 1 h, filtered by an organic filter membrane and analyzed by HPLC. The mobile phase was 25% acetonitrile–water (0.1% acetic acid), 0.8 mL min^{-1} flow rate, iso-elution, and the rest were the same as the HPLC condition of "2.5.1". The results were compared with the monosaccharide standard derivative products, and then the corresponding monosaccharide standard derivative products were added to the sample derivatives. After mixing, the HPLC analysis was performed again, and the D/L configuration of the sugar residue was finally determined.

2.5.4. Methylation analysis. The methylation experiment was proceeded according to the method described above with slight modifications.[16] Briefly, the dried polysaccharide sample (7 mg) was methylated with CH_3I three times and NaH in anhydrous DMSO. Subsequently, referring to the previously mentioned method,[18] we hydrolyzed, reduced and acetylated the methylated polysaccharides. The methylated alditol acetates were analyzed by GC-MS on a Thermo Fisher TRACE-1300 instrument with a TG-SQC column (15 m × 0.25 mm, 0.25 μm).

2.5.5. NMR. The 80 mg mL^{-1} polysaccharide sample solution was prepared by dissolving the dried polysaccharide sample in deuterium oxide (D_2O). A 500 MHz NMR spectrometer (AV-600, BRUKER, Germany) was employed to produce the ^1H NMR, ^{13}C NMR, ^1H–^1H COSY, HSQC and HMBC NMR spectra of RGP70-1-1 and RGP70-1-2.

2.5.6. Congo red experiment. RGP70-1-1 and RGP70-1-2 solutions (1 mg mL^{-1}) were mixed with Congo red solutions (100 mM) respectively, and then several gradient concentrations of sodium hydroxide solutions (0.00–0.60 M) were added. Ultraviolet scanning in the 400–600 nm wavelength range was carried out to identify the maximum absorption wavelength of each sample solution.

2.5.7. Scanning electron microscope analysis. The morphological characteristics of RG polysaccharides were observed by field emission scanning electron microscopy. A small amount of RGPs were uniformly dispersed on the conductive adhesive, and a layer of conductive gold film was sprayed on the surface of the polysaccharides in vacuum, then observed by scanning electron microscopy, adjusted magnification, and finally obtained a clear apparent morphology of the polysaccharides.[19]

2.6. Assay for α-glucosidase inhibitory activity

To ascertain the inhibitory effect of RGP70-1-1 and RGP70-1-2 on α-glucosidase, the method in related literature was adopted and slightly modified.[20] Firstly, the α-glucosidase solution was mixed with the sample solution and incubated for 5 min at 37 °C. The *p*NPG solution was subsequently added, and then reacted for 30 min at 37 °C. Lastly, the reaction was terminated by the addition of sodium carbonate, and the reactant's absorbance was measured at 405 nm.

2.7. Assay for α-amylase inhibition

To evaluate the inhibitory effect of RGP70-1-1 and RGP70-1-2 on α-amylase, the assay described in the literature was employed with certain modifications.[21] Briefly, the sample and α-amylase were incubated together at 37 °C for 10 min. Next, the starch solution was added and the reaction proceeded for 10 min at 37 °C. Then 125 μL of DNS reagent was added, the reaction proceeded for 5 min at 100 °C, then cooled to 25 °C and the absorbance at 540 nm was measured.

2.8. Cell line and cell culture

STC-1 cells were purchased from Shanghai Jinyuan Biotechnology Co., Ltd (Shanghai, China), cultured with DMEM containing 10% FBS and 1% penicillin-streptomycin solution and placed in an incubator in 5% CO_2 at 37 °C.

2.9. Cell viability

STC-1 cells were cultured in 96-well plates for 24 h (8000 cells per well), 100 μL of serum-free DMEM with RGP70-1-1 at various concentrations (0, 2×10^{-1}, 2×10^{-2}, 2×10^{-3}, 2×10^{-4}, 2×10^{-5}, 2×10^{-6} mM) were added after the culture medium had been removed. Then, 10 μL of CCK-8 solution was added to the reactant after 24 hours. At a wavelength of 450 nm, the absorbance was measured.

2.10. Measurements of GLP-1 secretion

STC-1 cells were treated with the RGP70-1-1(0, 0.02, 0.05, 0.1, 0.2 mM) previously dissolved in PBS for 2 h in 96-well plates. Then the supernatants from 96-well plates were centrifuged for 15 min at 1000×*g* and 4 °C, and collected. The assay of GLP-1 content was carried out using an ELISA kit (ml201801V, Shanghai Enzyme-Linked Biotechnology) according to the manufacturer's instructions. Taurocholate acid (TCA) was selected as the positive drug for cell experiments.

2.11. Western blot analysis

STC-1 cells were treated with RGP70-1-1 (0, 0.02, 0.05 mM) previously dissolved in PBS. The protein extraction and quantification were performed according to the methods reported in the literature.[22] An equal amount of 20 mg protein was electrophoresed on 10% SDS-page gels and transferred onto PVDF membranes. After blocking with 5% non-fat milk at room temperature, the membranes were incubated with primary antibodies (PI3K p110 Beta Polyclonal antibody, 20584-1-AP, Proteintech; Phospho-AKT (Ser473) Monoclonal antibody, 66444-1-Ig, Proteintech; GAPDH Monoclonal antibody, 60004-1-Ig, Proteinech) at 4 °C overnight. The membranes were washed five times with TBST buffer and then incubated with HRP-

conjugated secondary antibodies (HRP-conjugated Goat anti-Rabbit IgG(H + L), SA00001-2, Proteintech; HRP-conjugated Goat anti-Mouse IgG(H + L), SA00001-1, Proteintech). The blots were visualized by ECL kits, and the bands' density was quantified by ImageJ analysis software.

2.12. Statistical analysis

The experimental results are expressed as the mean ± standard deviation and analyzed using GraphPad Prism 9.5.1 (GraphPad, San Diego, CA, USA). Statistical analyses were performed by ANOVA. Comparisons that yielded p values < 0.05 were considered to indicate a statistically significant difference, and p values < 0.01 were considered very significant.

3 Results and discussion

3.1. Extraction, isolation and purification of RGP70-1-1 and RGP70-1-2

Polysaccharides are highly polar compounds generally extracted by hot water extraction.[23] Some methods for extracting polysaccharides include ultrasonic-assisted extraction, enzymatic extraction, and microwave-assisted extraction methods.[24–26] In this study, the crude polysaccharide RGP70 of RG was obtained using hot water extraction and the ethanol precipitation method, and was deproteinized and depigmented. RGP70 was separated by DEAE-Cellulose 52 and the eluate with high sugar content was collected to obtain RG70-1, RG70-2 and RG70-3, respectively (Fig. 1A). The RG70-1 was further eluted and purified by Sephacryl S-100 chromatography column. After the purity was verified by HPGPC, the polysaccharides with a uniform molecular weight distribution were collected, concentrated and freeze-dried. Two polysaccharides were obtained after Smur100 eluted RG70-1. The number of collecting tubes is shown in Fig. 1B, named RGP70-1-1 and RGP70-1-2. As shown in Table 1, the difference in the specific rotation values of the two precipitates of RGP70-1-1 and RGP70-1-2 is less than 5, indicating that these two polysaccharides are homogeneous.[27] The polysaccharides of RG were detected by the HPGPC method. RGP70-1-1 and RGP70-1-2 display a single peak, indicating that the two polysaccharides were homogeneous, consistent with the results of specific rotation. The molecular weights of RGP70-1-1 and RGP70-1-2 were determined by MALDI-TOF-MS because their molecular weights are outside the range of the dextran standard curve. The molecular weights of RGP70-1-1 and RGP70-1-2 are 4.9 kDa and 2.8 kDa (Fig. 1C–F), respectively.

3.2. Structural characterization of RGP70-1-1 and RGP70-1-2

3.2.1. Chemical composition analyses and D/L configuration analysis. Compared with the standard monosaccharide, it is shown that RGP70-1-1 and RGP70-1-2 are composed of four monosaccharides (mannose, glucose, galactose, and arabinose) (Fig. 2A–C). D/L configuration analysis can distinguish enantiomers and is one of the methods for characterizing polysaccharides. Compared to the retention times of monosaccharide standards with various configurations, the absolute configuration of mannose, glucose and galactose in RGP70-1-1 is D, and the absolute configuration of arabinose is L (Fig. 2D and E). The absolute configuration of mannose, glucose and galactose in RGP70-1-2 is D, and that of arabinose is L (Fig. 2F).

3.2.2. FT-IR spectrum analysis. To study molecules' structure and chemical bonds as a method for characterizing and

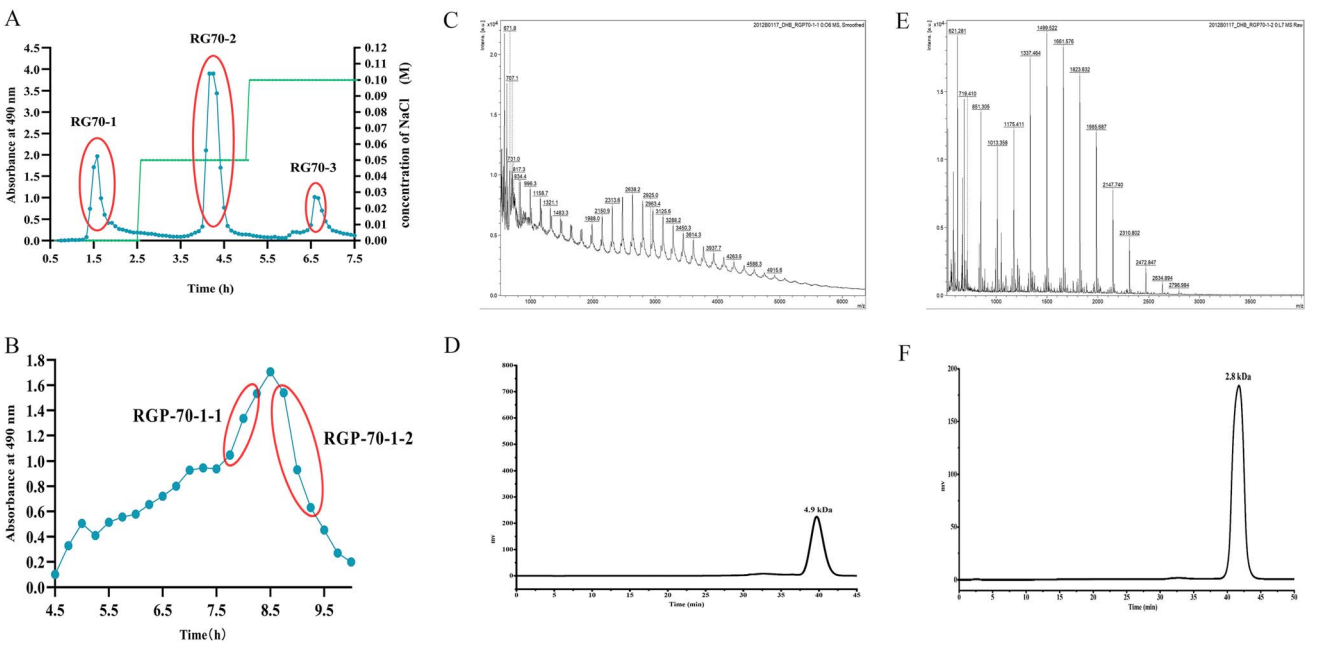

Fig. 1 Isolation and purification of RGP70-1-1 and RGP70-1-2. Elution curve of RG70 by DEAE-52 column chromatography (A), elution curve of RG70-1 by Sephacryl S-100 column chromatography (B), MALDI-TOF mass spectrum of RGP70-1-1 (C), the HPGPC chromatogram of RGP70-1-1 (D), MALDI-TOF mass spectrum of RGP70-1-2 (E) and the HPGPC chromatogram of RGP70-1-2 (F).

Table 1 The specific optical rotation analysis of polysaccharides from RG

Polysaccharide name	Specific rotation of precipitation I (c 0.1, H_2O)	Specific rotation of precipitation II (c 0.1, H_2O)
RGP70-1-1	$[\alpha]_D^{20} = -24.2$	$[\alpha]_D^{20} = -26.7$
RGP70-1-2	$[\alpha]_D^{20} = -20.0$	$[\alpha]_D^{20} = -17.3$

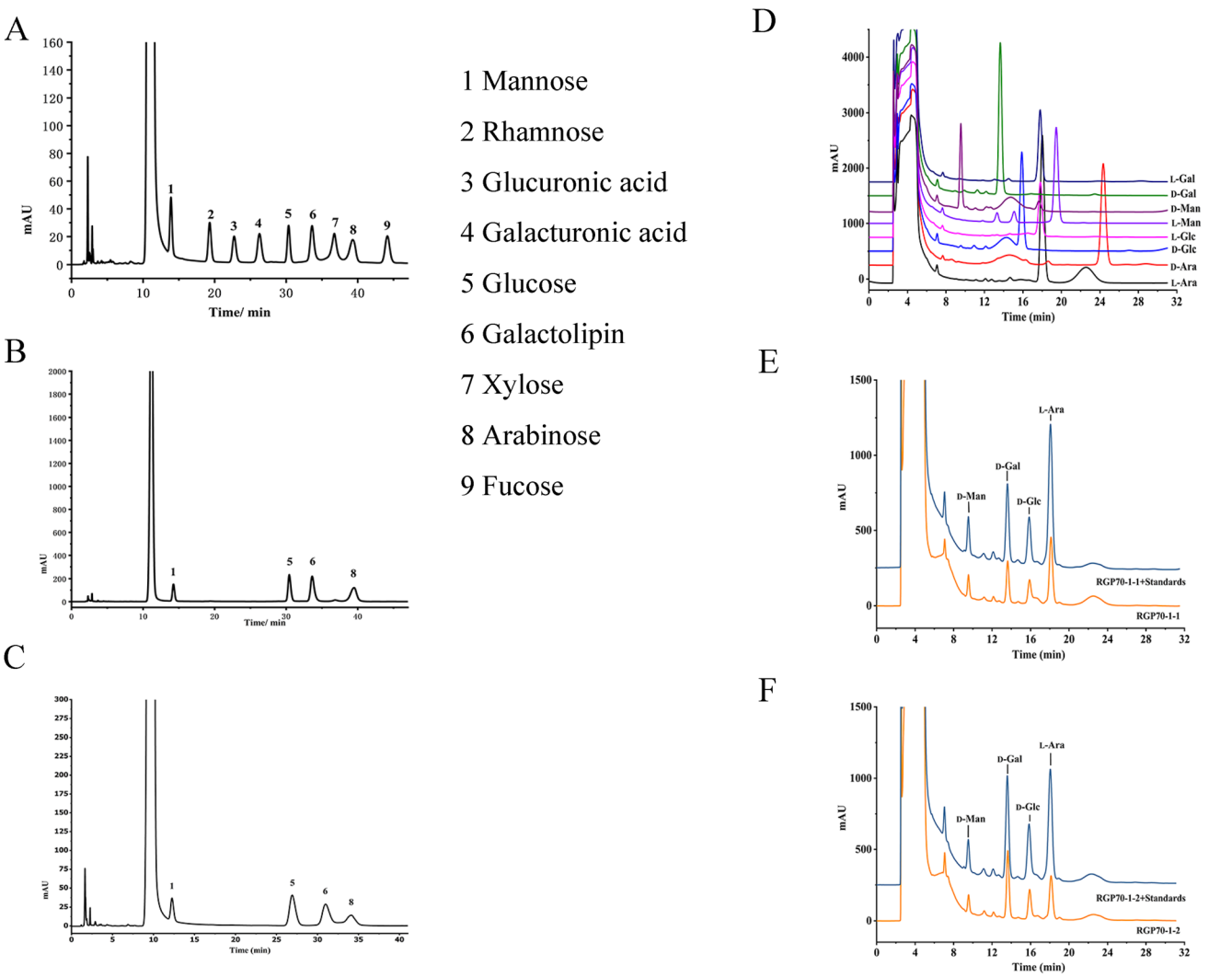

Fig. 2 HPLC chromatograms of PMP derivatives derived from monosaccharides, mixed monosaccharide standards (A), RGP70-1-1 hydrolysate (B), RGP70-1-2 hydrolysate (C). HPLC chromatograms of monosaccharide derivatives, monosaccharide standards (D), RGP70-1-1 hydrolysate (E), RGP70-1-2 hydrolysate (F).

identifying compounds, an infrared spectrum is performed to monitor the RGP70-1-1 and RGP70-1-2 (Fig. 3A and B). The infrared spectral characteristic absorption peaks of RGP70-1-1 and RGP70-1-2 are shown in Table S3.†

3.2.3. Methylation analysis. The infrared spectrometer detected the methylated RGP70-1-1 and RGP70-1-2. It was found that the hydroxyl characteristic peaks of RGP70-1-1 and RGP70-1-2 basically disappeared in the range of 3700–3200 cm^{-1} (Fig. 3C and D), which proved that RG70-1-1 and RGP70-1-2 were methylated completely and could be reduced and acetylated later.[28] Following the complete methylation of RGP70-1-1, the product was analyzed by GC-MS through complete acid hydrolysis, reduction and acetylation. As shown in Table S4,† 14 acetylated sugar alcohols were detected in the product. The relative proportion of retention time from small to large is 6.2 : 1.4 : 2.3 : 2.3 : 3.3 : 3.4 : 1.0 : 1.6 : 1.0 : 4.0 : 3.7 : 1.7 : 1.5 : 1.7. The results showed that RGP70-1-1 contains 14 connection modes, with the linkages including L-Ara$f$-(1→, →3)-L-Ara$f$-(1→, →5)-L-Ara$f$-(1→, →3,5)-L-Ara$f$-(1→, →2,5)-L-Ara$f$-(1→, D-Man$p$-(1→, →2)-D-Man$p$-(1→, →4)-D-Man$p$-(1→, D-Gal$p$-(1→, →4)-D-Gal$p$-(1→, →4,6)-D-Gal$p$-(1→,

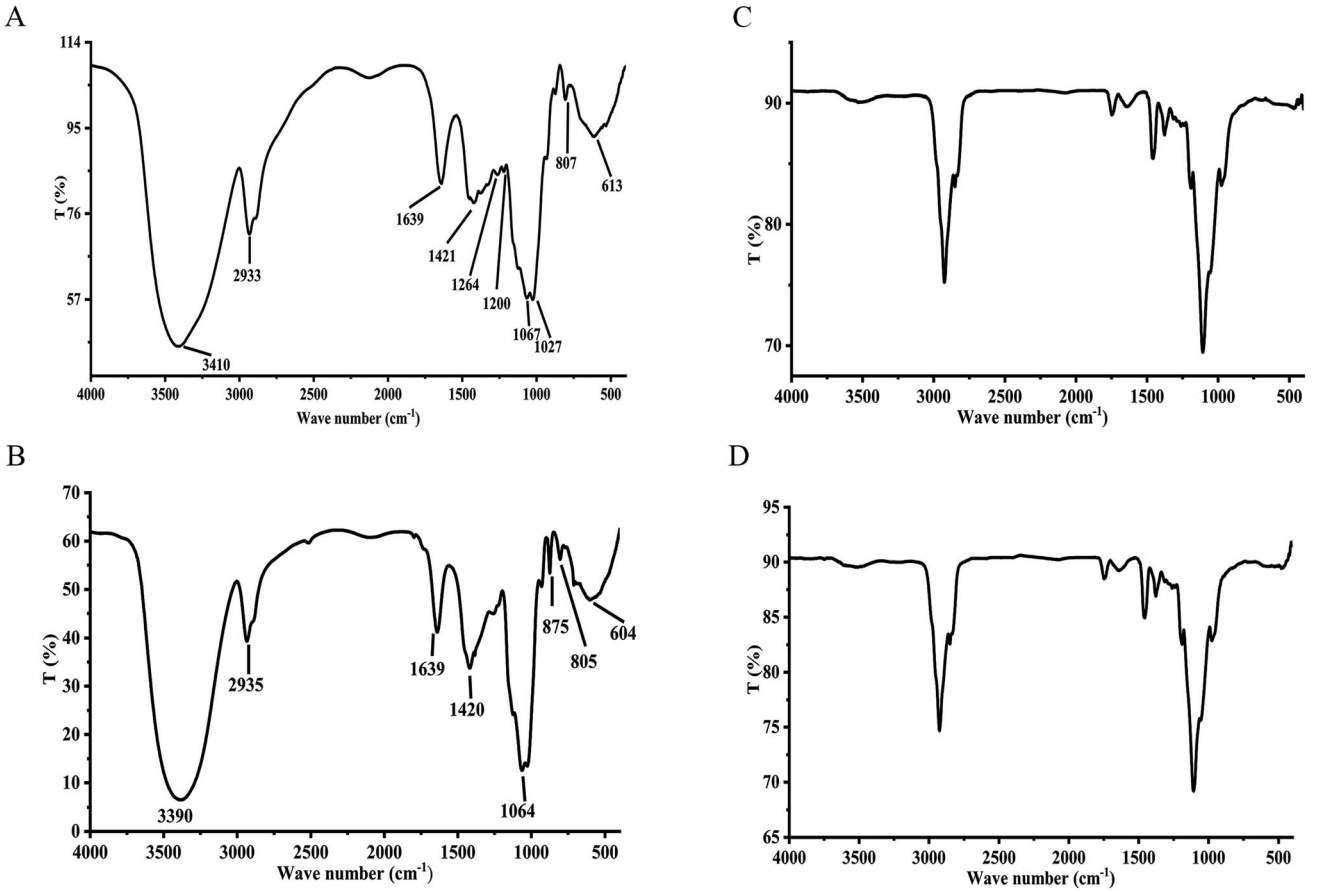

Fig. 3 Infrared spectrum of RGP70-1-1 (A), infrared spectrum of RGP70-1-2 (B), infrared spectrum of RGP70-1-1 after full methylation (C), infrared spectrum of RGP70-1-2 after full methylation (D).

→6)-D-Glc*p*-(1→, →4,6)-D-Glc*p*-(1→, →3,6)-D-Glc*p*-(1→. Once RGP70-1-2 is completely methylated, the product is analyzed by GC-MS as shown in Table S5.† Nine acetylated sugar alcohols are detected in the product. The relative ratio of retention time from small to large is 1.0 : 1.7 : 2.6 : 1.4 : 1.2 : 3.4 : 3.2 : 1.7 : 1.1. RGP70-1-2 consisted of mannose, glucose, galactose and arabinose, with linkages including →5)-L-Ara*f*-(1→, →3,5)-L-Ara*f*-(1→, →4)-D-Man*p*-(1→, →3,6)-D-Man*p*-(1→, D-Gal*p*-(1→, →6)-D-Gal*p*-(1→, D-Glc*p*-(1→, →6)-D-Glc*p*-(1→, →4,6)-D-Glc*p*-(1→.

3.2.4. NMR analysis. To reveal the chemical structure and sugar residues of RGP70-1-1, NMR spectroscopy is performed to analyze the structure of polysaccharides (Fig. 4). As can be seen from Fig. 4A, all the ^{1}HNMR peaks are between 1–6 ppm, which is a typical NMR spectrum of polysaccharides.[29]

From the HSQC spectrum, 14 terminal hydrogen and terminal carbon-related signals were observed, which were 5.07/107.1, 5.17/109.1, 5.00/107.4, 5.03/107.4, 5.17/107.0, 4.94/98.7, 5.00/98.5, 5.16/98.5, 4.40/103.2, 4.45/102.6, 4.44/103.1, 4.69/100.1, 4.68/100.1, 5.10/93.9 ppm, respectively labeled with sugar residues A, B, D, E, F, G, I, J, K, L, M, N, P, Q. The relative configuration of sugar is judged according to the chemical shift of terminal hydrogen, the coupling constant and the chemical shift of terminal carbon. Because the ratio of terminal carbon to β configuration of L-furan cyclic arabinose is in a low field, the sugar with a chemical shift of 107.1, 107.4, 107.0, 109.1 ppm in ^{13}C NMR spectrum is classified as L-furan cyclic arabinose with α configuration. The end group carbon of D-glucopyranose, D-galactose and D-mannose with isomorphic β configuration is in a low field, and $^3J_{H1,H2}$> 5 Hz, so D-galactose with chemical shifts of 103.1, 103.1, 102.6 ppm and D-glucopyranose with 100.1 ppm are assigned to β configuration, while the other six-carbon aldehydes belong to α configuration.

The chemical shift of H2 is determined according to its correlation with H-1.[30] According to relevant reference books, literature reports and resonance peaks on ^{1}H–^{1}H COSY spectrum δ_H 5.07/4.05, the H2 signal of residue A is estimated to 4.05 ppm. Similarly, according to the good correlation between H2 and H3, combined with the chemical signal on ^{1}H–^{1}H COSY spectrum, H3 of residue A is classified as δ_H 3.89, δ_H 3.89/3.88 belongs to H3/H4 of residue A, while H5 is determined according to the signal strength of ^{1}H NMR spectrum, and then the C and H signals of residue A are assigned in combination with ^{13}C NMR and HSQC spectrum. The relevant peaks are 5.07/107.1, 4.05/81.2, 3.89/76.5, 3.88/83.4, 3.74/61.2, 3.75/61.2 ppm, respectively, corresponding to H1/C1, H2/C2, H3/C3, H4/C4, H5/C5 of residue A; similarly, for residue B, the resonance peak on ^{1}H–^{1}H COSY spectrum δ_H 5.17/4.03, δ_H 4.03/3.79 corresponds to H1/H2 and H2/H3 respectively. C3 on furan

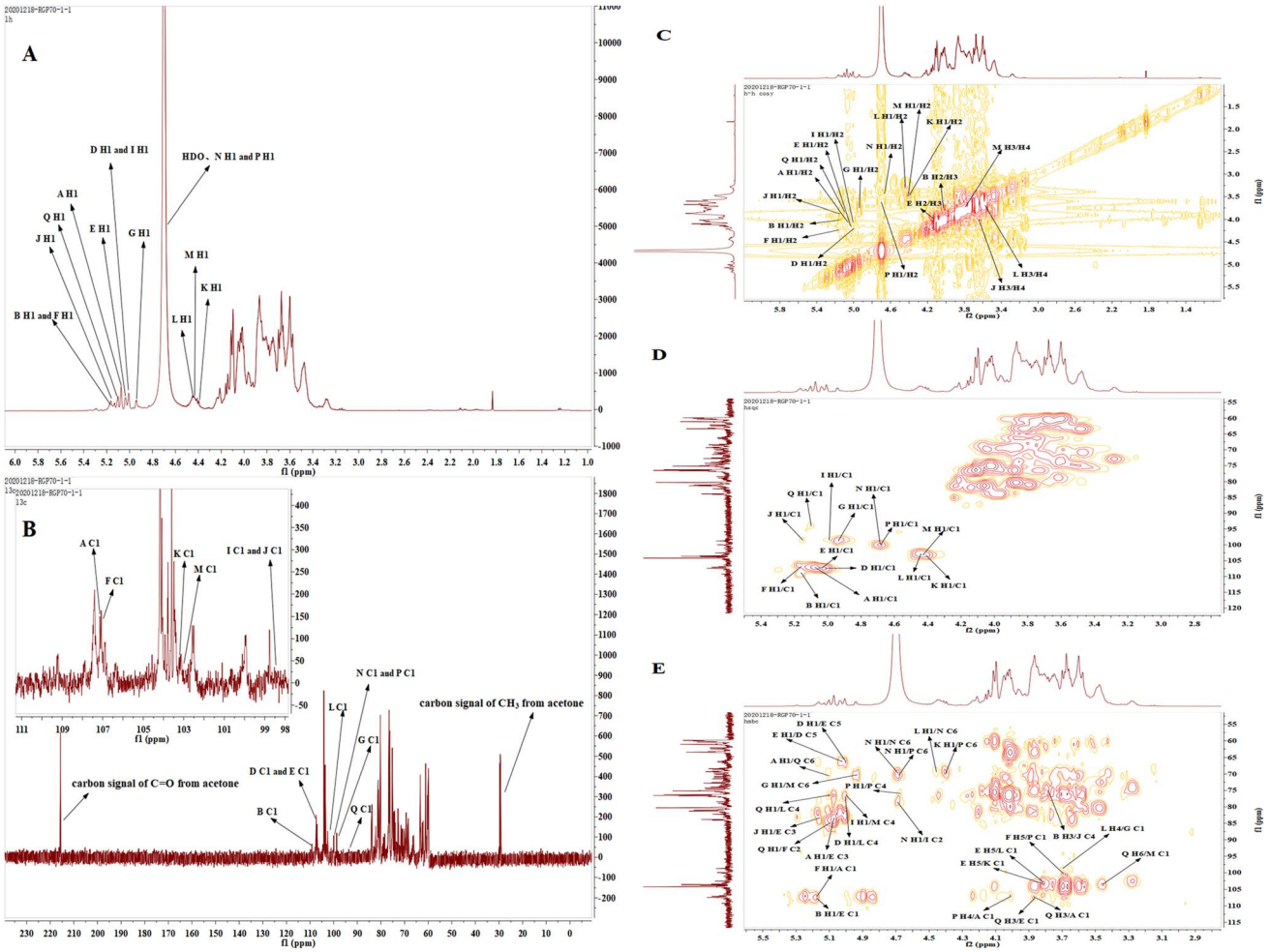

Fig. 4 ^{1}H-NMR (A), ^{13}C-NMR (B), ^{1}H–^{1}H COSY (C), HSQC (D) and HMBC (E) spectra of RGP70-1-1.

arabinose is replaced and C3 chemical shift δ moving to the low field, combining with the HSQC spectrum, we can infer that the H3/C3 chemical shift of residue B is 3.79/81.4 ppm, while H4 and C3 have good correlation, combining with the resonance signal 3.95/81.4 ppm on the HMBC spectrum, we can infer that the chemical shift of H4 is 3.95 ppm, combining with 1H NMR and HSQC spectrum, we can assign the C and H signals of residue B, and the correlation peaks are 5.17/109.1, 4.03/81.4, 3.79/81.4, 3.95/84.1, 3.76/61.4, 3.78/61.4 ppm respectively corresponding to the H1/C1, H2/C2, H3/C3, H4/C4, H5/C5 of residue B; it can be inferred from the same method that the relevant peaks 5.00/107.4, 4.21/81.4, 3.73/76.6, 4.01/83.1, 3.74/66.2, 3.70/66.2 ppm respectively correspond to the H1/C1, H2/C2, H3/C3, H4/C4, H5/C5 of residue D; relevant peaks 5.03/107.4, 4.14/81.8, 3.97/83.8, 3.96/83.9, 3.87, 3.82/66.4 ppm respectively correspond to H1/C1, H2/C2, H3/C3, H4/C4, H5/C5 of residue E; relevant peaks 5.17/107.0, 4.24/85.0, 3.72/76.8, 3.97/83.7, 3.66/66.6, 3.69/66.6 ppm respectively correspond to H1/C1, H2/C2, H3/C3, H4/C4, H5/C5 of residue F; relevant peaks 4.94/98.7, 3.74/71.2, 3.72/72.1, 3.80/68.1, 3.83/73.8, 3.82/63.2, 3.81/63.2 ppm respectively correspond to H1/C1, H2/C2, H3/C3, H4/C4, H5/C5, H6/C6 of residue G; relevant peaks 5.00/98.5, 4.06/78.9, 3.69/71.6, 3.75/68.7, 3.59/73.7, 3.56, 3.57/62.8 ppm respectively correspond to H1/C1, H2/C2, H3/C3, H4/C4, H5/C5, H6/C6 of residue I; relevant peaks 5.16/98.5, 3.87/72.1, 3.64/72.5, 4.01/75.2, 3.61/73.8, 3.57/62.7, 3.56/62.7 ppm respectively correspond to H1/C1, H2/C2, H3/C3, H4/C4, H5/C5, H6/C6 of residue J; relevant peaks 4.40/103.2, 3.47/71.1, 3.79/74.0 3.87/69.5, 3.77/76.6, 3.49/63.3, 3.48/63.3 ppm respectively correspond to H1/C1, H2/C2, H3/C3, H4/C4, H5/C5, H6/C6 of residue K; relevant peaks 4.45/102.6, 3.28/72.8 3.60/73.8, 3.70/76.6, 3.73/76.7, 3.49/63.4, 3.48/63.4 ppm respectively correspond to H1/C1, H2/C2, H3/C3, H4/C4, H5/C5, H6/C6 of residue L; relevant peaks 4.44/103.1, 3.54/71.2, 3.80/73.9, 3.73/76.5, 3.88/76.5, 3.58/70.1, 3.59/70.1 ppm respectively correspond to H1/C1, H2/C2, H3/C3, H4/C4, H5/C5, H6/C6 of residue M; relevant peaks 4.69/100.1, 3.42/75.6, 3.65/76.4, 3.72/71.5, 4.11/76.3, 3.87/69.3, 3.89/69.3 ppm respectively correspond to H1/C1, H2/C2, H3/C3, H4/C4, H5/C5, H6/C6 of residue N; relevant peaks 4.68/100.1, 3.61/74.1, 3.62/76.4, 4.02/75.4, 3.96/76.4, 3.86/69.6, 3.88/69.6 ppm respectively correspond to H1/C1, H2/C2, H3/C3, H4/C4, H5/C5, H6/C6 of residue P; relevant peaks 5.10/93.9, 3.85/73.7, 3.88/80.3, 3.48/70.9, 3.85/73.8, 3.47/70.8, 3.48/70.8 ppm respectively correspond to H1/C1,

H2/C2, H3/C3, H4/C4, H5/C5, H6/C6 of residue Q. As the shown in Table S6† for the attribution results of C and H signals in ^{13}C NMR spectrum No obvious chemical signals were observed within δ 170–180 ppm, indicating that the polysaccharide is free of uronic acid, which corresponded to the composition of the monosaccharide.

We analyzed the linkage sites and the sequence between the sugar residues according to the resonance peak in the HMBC spectrum. The correlation peak 5.07 (A H1)/83.8 ppm (E C3) indicates that the O-1 of residue A is connected with C-3 of residue E; similarly, the correlation peak 3.82(E H5)/103.2 ppm (K C1) indicates that the O-5 of residue E is connected with C-1 of residue K; the correlation peak 5.03 (E H1)/66.2 ppm (D C5) indicates that the O-1 of residue E is connected to the C-5 of residual D; the correlation peak 5.00(D H1)/66.4 ppm (E C5) indicates that the O-1 of residue D is connected to the C-5 of residue E; the correlation peak 5.17(B or F H1)/107.4 ppm (E C1) indicates that the O-1 of residue B or residue F is connected to the C-1 of residue E; the correlation peak 3.79(B H3)/75.2 ppm (J C4) indicates that the O-3 of residue B is connected with C-4 of residue J; the correlation peak 5.16(J H1)/83.8 ppm (E C3) indicates that the O-1 of residue J is connected with C-3 of residue E; the correlation peak of 5.00(D H1)/76.6 ppm (L C4) indicates that the O-1 of residue D is connected with C-4 of residue L; the correlation peak 3.69 (F H5)/100.1 ppm (P C1) indicates that the O-5 of residue F is connected with C-1 of residue P; the correlation peak 3.88(Q H3)/107.4 ppm (E C1) indicates that the O-3 of residue Q is connected with C-1 of residue E; the correlation peak 4.45(L H1)/69.3 ppm (N C6) indicates that the O-1 of residue L is connected with C-6 of residue N; the correlation peak 4.69(N H1)/69.3 ppm (N C6) indicates that the O-1 of residue N is connected to the C-6 of residue N, indicating that there is a duplicate unit residue N; the correlation peak 4.69(N H1/)/69.6 ppm (P C6) indicates that the O-1 of residue N is connected with C-6 of residue P; the correlation peak 4.69(N H1)/78.9 ppm (I C2) indicates that the O-1 of residue N is connected to the C-2 of residual I; the correlation peak 3.82(E H5)/102.6 ppm (L C1) indicates that the O-5 of residue E is connected with C-1 of residue L; the correlation peak of 5.00(I H1)/76.5 ppm (M C4) indicates that the O-1 of residue I is connected with C-4 of residue M; the correlation peak 3.70(L H4)/98.7 ppm (G C1) indicates that the O-4 of residue L is connected with C-1 of residue G; the correlation peak 3.47 (Q H6)/103.1 ppm (M C1) indicates that the O-6 of residue Q is connected with C-1 of residue M; the correlation peak 4.94 (G H1)/70.1 ppm (M C6) indicates that the O-1 of residue G is connected with C-6 of residue M; the correlation peak 5.10 (Q H1)/85.0 ppm (F C2) indicates that the O-1 of residue Q is connected to the C-2 of residue F; the correlation peak 5.17 (F H1)/107.1 ppm (A C1) indicates that the O-1 of residue F is connected to the C-1 of residue A; the correlation peak 4.02 (P H4)/107.1 ppm (A C1) indicates that the O-4 of

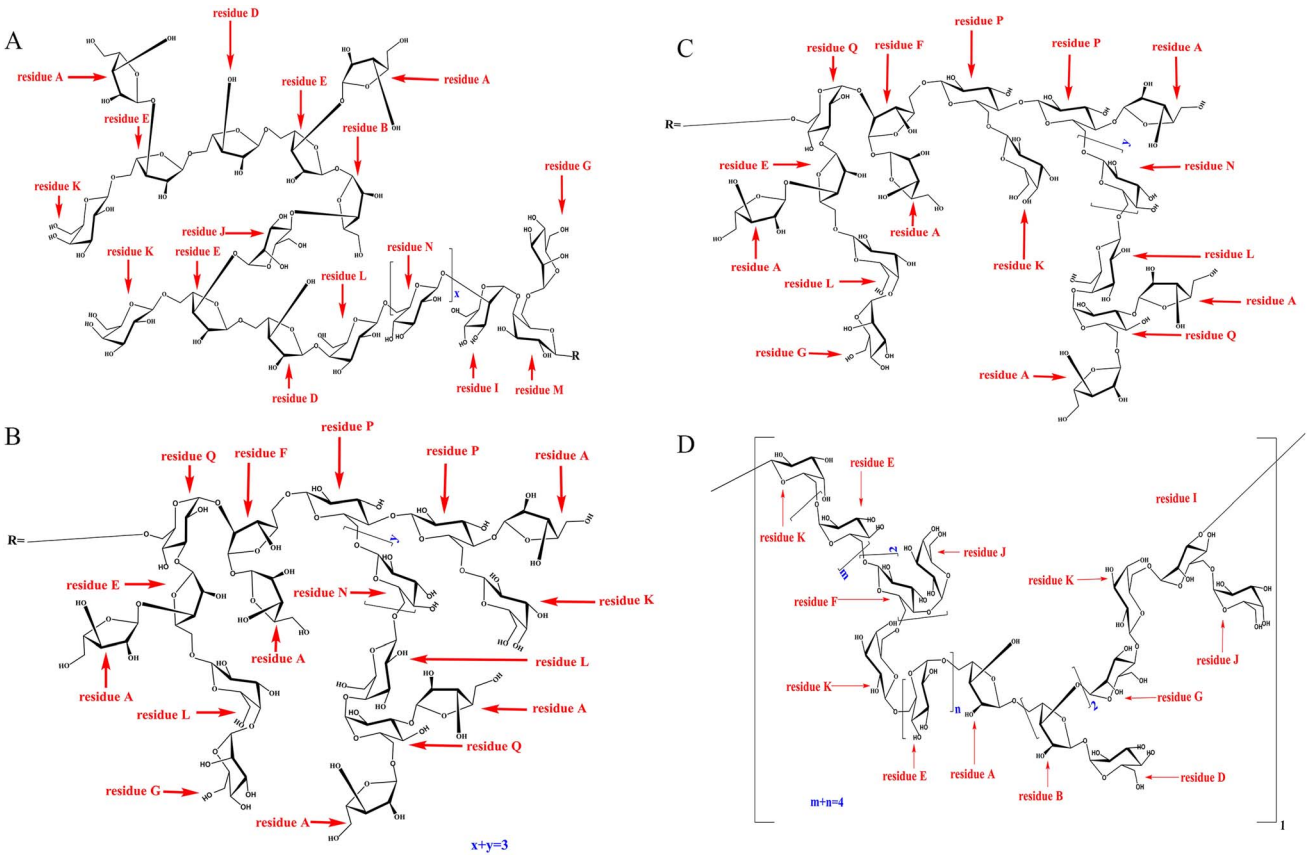

Fig. 5 The structure of the repeating unit of RGP70-1-1 (A), (B) and (C), the structure of the repeating unit of RGP70-1-2 (D).

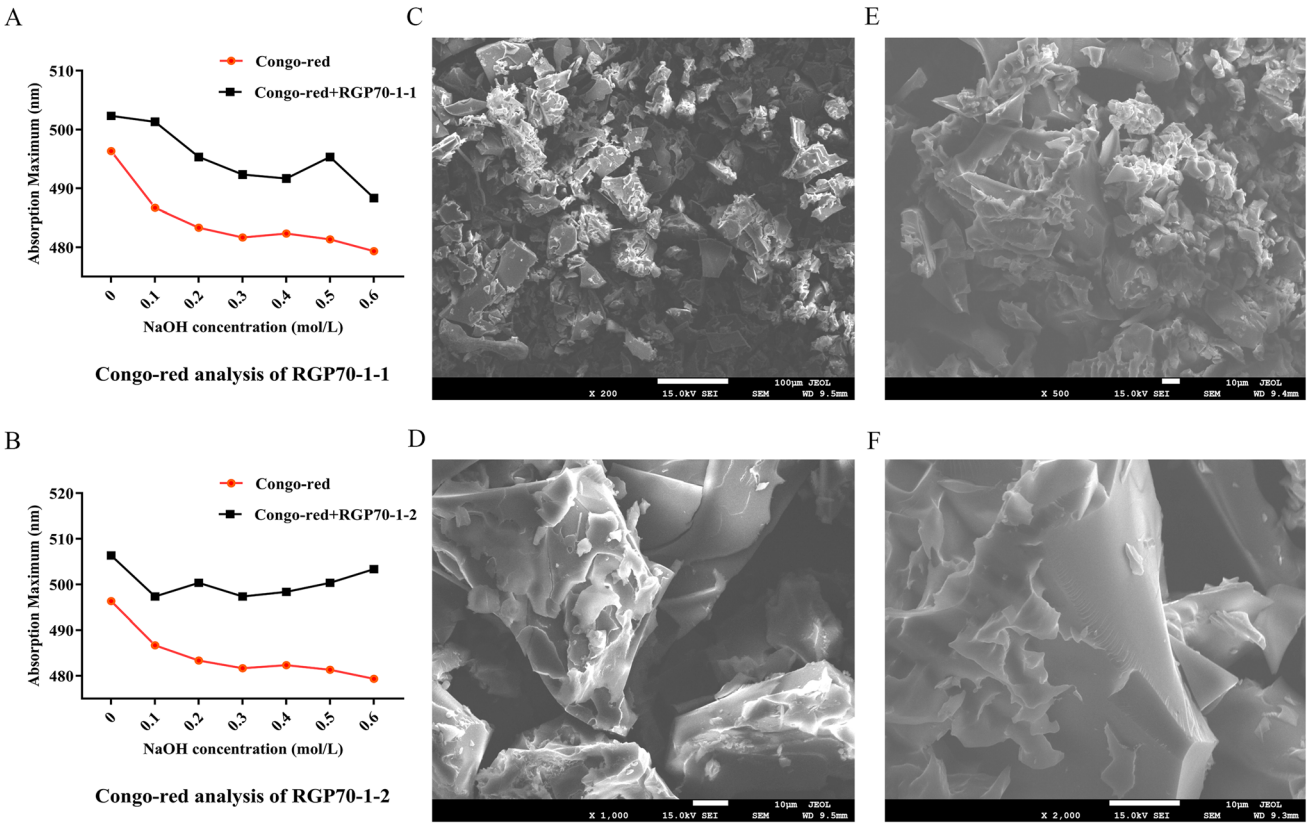

Fig. 6 Congo-red analysis of RGP70-1-1 (A), Congo-red analysis of RGP70-1-2 (B), scanning electronic micrograph for RGP70-1-1 (C and D referring to the images of RGP70-1-1 at magnifications of 200×, 1000×), Scanning electronic micrograph for RGP70-1-2 (E and F referring to the images of RGP70-1-2 at magnifications of 500×, 2000×).

residue P is connected with C-1 of residue A; the correlation peak 4.40 (K H1)/69.6 ppm (P C6) indicates that the O-1 of residue K is connected with C-6 of residue P; the correlation peak 5.10 (Q H1)/76.6 ppm (L C4) indicates that the O-1 of residue Q is connected to the C-4 of residue L; the correlation peak 5.10 (A H1)/70.8 ppm (Q C6) indicates that the O-1 of residue A is connected with C-6 of residue Q; the correlation peak 3.88 (Q H3)/107.1 ppm (A C1) indicates that O-3 of residue Q is connected with C-1 of residue A; the correlation peak 4.68 (P H1)/75.4 ppm (P C4) indicates that the O-1 of the residue P is connected to the C-4 of the residue P.

Similar to RGP70-1-1, the structure of RGP70-1-2 can be determined using the above methods and spectral information (Fig. S1 and Table S7†).

Through structural characterization and analysis, the primary structure of RGP70-1-1 was inferred. The results showed a polysaccharide composed of arabinose, glucose, mannose and galactose. RGP70-1-2 is a polysaccharide composed of arabinose, glucose, mannose and galactose. The structural repeating units of RGP70-1-1 and RGP70-1-2 are shown in Fig. 5.

3.2.5. Congo red and SEM analysis. The purpose of the Congo red test is to verify whether the compound contains a triple helix structure. With the increase in sodium hydroxide concentration, the maximum absorption wavelength of RGP70-1-1 decreases at first, then increases, and finally decreases, which is not consistent with the special change in triple helix structure reaction, indicating that RGP70-1-1 has no triple helix structure (Fig. 6A). The maximum absorption wavelength of RGP70-1-2 decreased at first, then increased and then decreased, and finally showed an upward trend, which was not consistent with the special change in triple helix structure, indicating that RGP70-1-2 had no triple helix structure (Fig. 6B). The surface microstructure and aggregation morphology of polysaccharides were provided by a scanning electron microscope (SEM). As shown from Fig. 6C and D, RGP70-1-1 is irregularly fragmented, with a layer of white wax on the edge, scattered distribution and a smooth surface. RGP70-1-2 is an irregular broken block; the edge is like a layer of white wax, with scattered distribution. Local magnification can show that its surface is smooth (Fig. 6E and F).

3.3. Hypoglycemic effects of RGP70-1-1 and RGP70-1-2 *in vitro*

3.3.1. Assay for α-glucosidase and α-amylase inhibition. Inhibition of carbohydrate hydrolases, such as α-glucosidase and α-amylase, is one of the primary strategies for reducing postprandial hyperglycemia.[31] Acarbose as a type of sugar α-glucosidase inhibitor can slow down glucose absorption and alleviate postprandial hyperglycemia.[32] Therefore, the hypoglycemic properties of RGP70-1-1 and RGP70-1-2 were determined

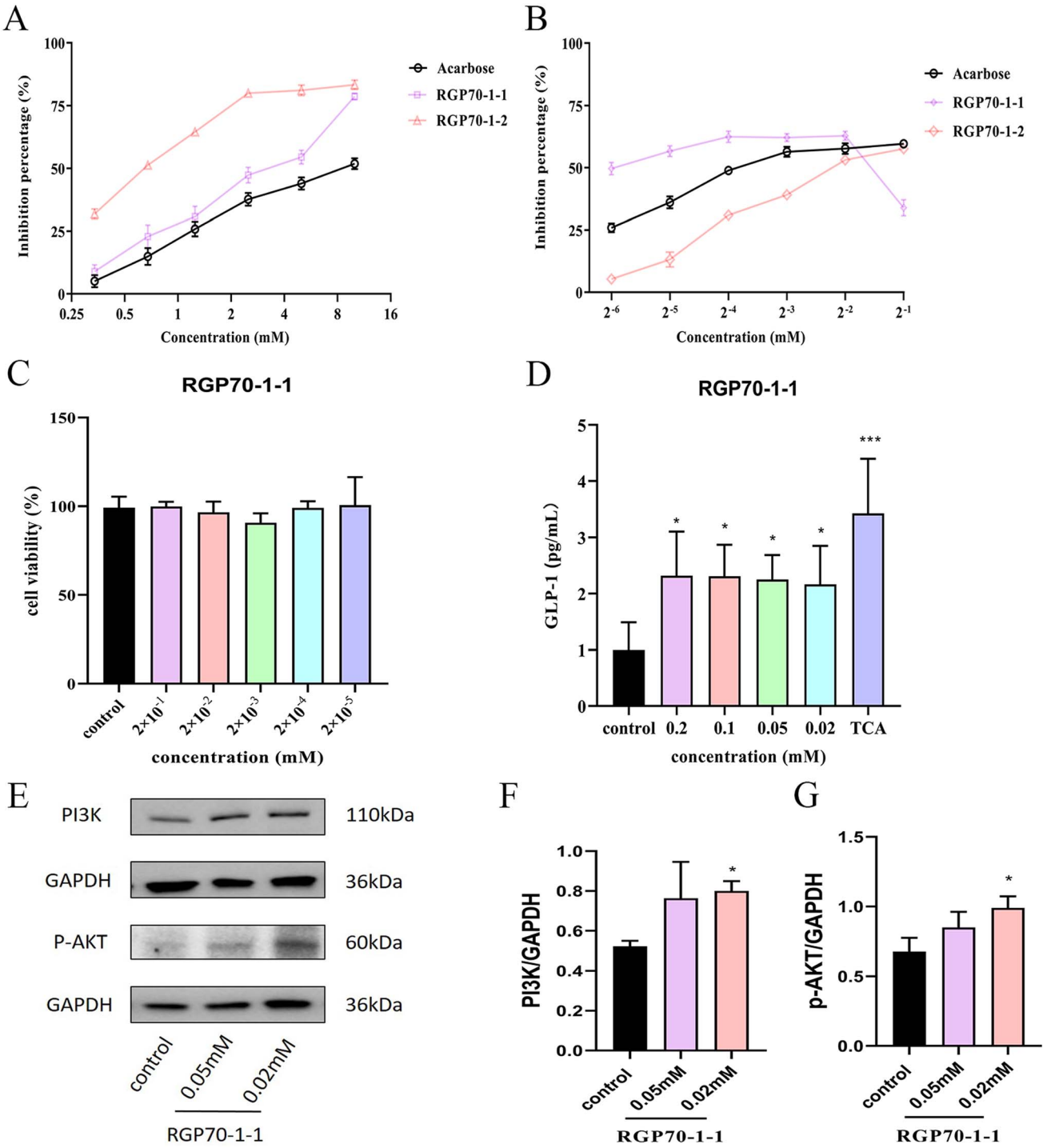

Fig. 7 Inhibition of α-glucosidase activity by RGP70-1-1 and RGP70-1-2 (A), inhibition of α-amylase activity by RGP70-1-1 and RGP70-1-2 (B), cell viability after treatment of STC-1 cells with RGP70-1-1 for 24 h (C), different concentrations of RGP70-1-1 on GLP-1 secretion by STC-1 cell (D), detection of the effect of RGP70-1-1 on the protein levels of PI3K and p-AKT in STC-1 cells by western-blot (E), the protein levels of PI3K/GAPDH (F) and p-AKT/GAPDH (G) were detected by the Wester-blot ($n = 3$). *$p < 0.05$, **$p < 0.01$ compared with the control group.

by evaluating the inhibitory activity of α-glucosidase and α-amylase *in vitro* (Fig. 7A and B). With the increase in concentration, the inhibitory effect of acarbose, RGP70-1-2 and RGP70-1-1 on α-glucosidase activity was stronger. The inhibitory effect of RGP70-1-2 and RGP70-1-1 on α-glucosidase activity was stronger than that of acarbose. Both RGP70-1-1 and RGP70-1-2 could inhibit α-amylase activity. The inhibitory effect of RGP70-1-1 on α-amylase activity was stronger than that of acarbose. The results showed that RGP70-1-1 and RGP70-1-2 had potential hypoglycemic activity.

3.3.2. Effects of RGP70-1-1 on the GLP-1 secretion *via* PI3K/AKT signaling pathway in RGP70-1-1-induced STC-1 cells. From the perspective of enzyme activity, it is found that RGP70-1-1 has good hypoglycemic activity. Therefore, we continue to explore the hypoglycemic activity of RGP70-1-1 on the cellular level. GLP-1 released by intestinal enteroendocrine cells monitors meal-related blood glucose excursions through increased insulin and inhibition of glucagon secretion.[6] The STC-1 is a murine enteroendocrine cell line routinely used to test the secretion of GLP-1 *in vitro*.[33] At present, many polysaccharides have a variety of pharmacological effects, especially hypoglycemic effects without allergic reactions, such as *Dendrobium officinale.* polysaccharides[18] and *Cyclocarya paliurus* polysaccharides.[34] TCA has been reported to promote GLP-1 secretion, so TCA was selected as a positive drug.[35] In this study, the polysaccharides we obtained also showed the effect of promoting the secretion of STC-1. As shown in Fig. 7D, treatment with RGP70-1-1 distinct augments the release of GLP-1 in all dosages tested. PI3K/AKT, as a serine/threonine protein kinase, plays an essential role in modulating insulin to signal glucose metabolism.[36] It has been reported that GLP-1 secretion is related to the PI3K/AKT signal pathway.[37] To assess whether RGP70-1-1 stimulates the PI3K/Akt pathway, the expression levels of PI3K/Akt were measured by western blot. After RGP70-1-1 administration, the expressions of PI3K and p-AKT were significantly elevated (Fig. 7E–G). The results suggest that RGP70-1-1 promotes GLP-1 secretion by STC-1 cells, which may be related to the up-regulation of PI3K and p-AKT expression. RGP, as a natural product with low toxic side effects, may be developed into a new hypoglycemic drug or functional food to promote STC-1 secretion in diabetes patients.

4 Conclusions

In the present study, two novel polysaccharides (RGP70-1-1 and RGP70-1-2) were separated from *Rehmannia glutinosa* Libosch. RGP70-1-1 was composed of L-Ara*f*-(1→, →3)-L-Ara*f*-(1→, →5)-L-Ara*f*-(1→, →3,5)-L-Ara*f*-(1→, →2,5)-L-Ara*f*-(1→, D-Man*p*-(1→, →2)-D-Man*p*-(1→, →4)-D-Man*p*-(1→, D-Gal*p*-(1→, →4)-D-Gal*p*-(1→, →4,6)-D-Gal*p*-(1→, →6)-D-Glc*p*-(1→, →4,6)-D-Glc*p*-(1→, →3,6)-D-Glc*p*-(1→, with molecular weights of 4.9 kDa. RGP70-1-2 were composed of →5)-L-Ara*f*-(1→, →3,5)-L-Ara*f*-(1→, →4)-D-Man*p*-(1→, →3,6)-D-Man*p*-(1→, D-Gal*p*-(1→, →6)-D-Gal*p*-(1→, D-Glc*p*-(1→, →6)-D-Glc*p*-(1→, →4,6)-D-Glc*p*-(1→, with molecular weights of 2.8 kDa. RGP70-1-1 and RGP70-1-2 can inhibit α-amylase and α-glucosidase activity. Further *in vitro* experiments showed that GLP-1 secretion was proven to be stimulated by RGP70-1-1 in STC-1 cells. Furthermore, intracellular RGP70-1-1-induced GLP-1 secretion may be mediated by the PI3K/AKT pathways. These findings imply that RGP70-1-1 may have a hypoglycemic impact and potentially develop into new hypoglycemic medications or health food. It may help to develop new medication for the treatment of T2D and improve the utilization rate of RG. Therefore, RGP70-1-1 has potential applications in the pharmaceutical and food industries.

Abbreviations

COSY	Correlation spectroscopy
DPP-4	Dipeptidyl peptidase 4
FT-IR	Fourier-transform infrared
GC-MS	Gas chromatography-mass spectrometer
GLP-1	Glucagon-like peptide-1
HPGPC	High-performance gel permeation chromatography
HPLC	High performance liquid chromatography
HMBC	Heteronuclear multiple bond spectroscopy
HSQC	Heteronuclear single quantum coherence spectroscopy
MALDI-TOF-MS	Matrix-assisted laser desorption ionization time-of-flight mass spectrometry
NMR	Nuclear magnetic resonance
PMP	1-Phenyl-3-methyl-5-pyrazolone
*p*NPG	*p*-Nitrophenyl-α-D-glucoside
SEM	Scanning electron microscope
T2D	Type 2 diabetes
TFA	Trifluoroacetic acid
TCA	Taurocholate acid

Author contributions

Huien Chen: data curation, methodology, software, writing – original draft, writing – review & editing. Xinyu Liu: data curation, investigation, software. Meixia Xie: data curation, investigation, software. Xiaoting Zhong: conceptualization, data curation, investigation, software, visualization. Chunyan Yan: conceptualization, methodology, data curation, investigation, software. Minghua Xian: conceptualization, funding acquisition, methodology, project administration, supervision, writing – review, editing, and writing – original draft. Shumei Wang: conceptualization, funding acquisition, methodology, project administration, supervision, writing – review, editing, and writing – original draft.

Conflicts of interest

The authors declare no conflict of interest.

Acknowledgements

This work was supported by National Natural Science Foundation of China (grant numbers 82173972, 81773884) and Guangdong Basic and Applied Basic Research Foundation (grant numbers 2023A1515011147).

References

1 H. Sun, P. Saeedi, S. Karuranga, M. Pinkepank, K. Ogurtsova, B. B. Duncan, C. Stein, A. Basit, J. C. N. Chan, J. C. Mbanya, M. E. Pavkov, A. Ramachandaran, S. H. Wild, S. James, W. H. Herman, P. Zhang, C. Bommer, S. Kuo, E. J. Boyko and D. J. Magliano, *Diabetes Res. Clin. Pract.*, 2022, **183**, 109119.

2 S. E. Kahn, R. L. Hull and K. M. Utzschneider, *Nature*, 2006, **444**, 840–846.
3 D. de Paulo Farias, F. F. de Araújo, I. A. Neri-Numa and G. M. Pastore, *Food Res. Int.*, 2021, **145**, 110383.
4 J. J. Meier, *Nat. Rev. Endocrinol.*, 2012, **8**, 728–742.
5 K. Pabreja, M. A. Mohd, C. Koole, D. Wootten and S. G. B. Furness, *Br. J. Pharmacol.*, 2014, **171**, 1114–1128.
6 D. J. Drucker, *Cell Metab.*, 2018, **27**, 740–756.
7 D. J. Drucker and M. A. Nauck, *Lancetc*, 2006, **368**, 1696–1705.
8 M. Li, H. Jiang, Y. Hao, K. Du, H. Du, C. Ma, H. Tu and Y. He, *J. Ethnopharmacol.*, 2022, **285**, 114820.
9 Z. Bian, R. Zhang, X. Zhang, J. Zhang, L. Xu, L. Zhu, Y. Ma and Y. Liu, *J. Ethnopharmacol.*, 2023, **305**, 116132.
10 R. Zhang, J. Zhou, Z. Jia, Y. Zhang and G. Gu, *J. Ethnopharmacol.*, 2004, **90**, 39–43.
11 B. Zhang, M. Zeng, Y. Wang, M. Li, Y. Wu, R. Xu, Q. Zhang, J. Jia, Y. Huang, X. Zheng and W. Feng, *Phytomedicine Int. J. Phytother. Phytopharm.*, 2022, **94**, 153818.
12 Y. Duan, Y. Huang, G. Wei and D. Liu, *J. Shaanxi Univ. Chin. Med.*, 2013, **36**, 110–112.
13 Y. Yu, M. Shen, Q. Song and J. Xie, *Carbohydr. Polym.*, 2018, **183**, 91–101.
14 J. Zhou, G. Xu, J. Yan, K. Li, Z. Bai, W. Cheng and K. Huang, *J. Ethnopharmacol.*, 2015, **164**, 229–238.
15 L. Guo, H. Dai, J. Ma, J. Wang, Y. Hua and L. Zhou, *BMC Chem.*, 2021, **15**, 19.
16 X. Ji, Y. Yan, C. Hou, M. Shi and Y. Liu, *Int. J. Biol. Macromol.*, 2020, **147**, 844–852.
17 P.-X. Gong, Y.-C. Wu, Y. Liu, S.-Z. Lv, Y. You, Z.-L. Zhou, X. Chen and H.-J. Li, *Int. J. Biol. Macromol.*, 2022, **216**, 14–23.
18 M.-T. Kuang, J.-Y. Li, X.-B. Yang, L. Yang, J.-Y. Xu, S. Yan, Y.-F. Lv, F.-C. Ren, J.-M. Hu and J. Zhou, *Carbohydr. Polym.*, 2020, **241**, 116326.
19 X. Liu, Z. Ren, R. Yu, S. Chen, J. Zhang, Y. Xu, Z. Meng, Y. Luo, W. Zhang, Y. Huang and T. Qin, *Int. J. Biol. Macromol.*, 2021, **166**, 1396–1408.
20 J. Song, Y. Wu, X. Ma, L. Feng, Z. Wang, G. Jiang and H. Tong, *Carbohydr. Polym.*, 2020, **230**, 115586.
21 C. Wang, W. Li, Z. Chen, X. Gao, G. Yuan, Y. Pan and H. Chen, *Food Res. Int. Ott. Ont*, 2018, **103**, 280–288.
22 J. Cai, J. Liang, Y. Zhang, L. Shen, H. Lin, T. Hu, S. Zhan, M. Xie, S. Liang, M. Xian and S. Wang, *Pharmacol. Res.*, 2022, **180**, 106230.
23 P. Zeng, J. Li, Y. Chen and L. Zhang, *Prog. Mol. Biol. Transl. Sci.*, 2019, **163**, 423–444.
24 N. A. Al-Dhabi and K. Ponmurugan, *Int. J. Biol. Macromol.*, 2020, **152**, 1157–1163.
25 J. Nai, C. Zhang, H. Shao, B. Li, H. Li, L. Gao, M. Dai, L. Zhu and H. Sheng, *Int. J. Biol. Macromol.*, 2021, **183**, 2337–2353.
26 C. Yun, X. Ji, Y. Chen, Z. Zhao, Y. Gao, L. Gu, D. She, I. Ri, W. Wang and H. Wang, *Int. J. Biol. Macromol.*, 2023, **227**, 134–145.
27 Z. Zeng, X. Chang, D. Zhang, H. Chen, X. Zhong, Y. Xie, Q. Yu and C. Yan, *Int. J. Biol. Macromol.*, 2022, **219**, 1284–1296.
28 J. Chen, L. Li, X. Zhou, B. Li, X. Zhang and R. Hui, *Int. J. Biol. Macromol.*, 2018, **117**, 815–819.
29 J. Liu, Y. Li, Q. Pu, H. Qiu, D. Di and Y. Cao, *Int. J. Biol. Macromol.*, 2022, **201**, 111–120.
30 X. Ji, F. Liu, Q. Peng and M. Wang, *Food Chem.*, 2018, **245**, 1124–1130.
31 H. Zhang, J. Zhao, H. Shang, Y. Guo and S. Chen, *Int. J. Biol. Macromol.*, 2020, **148**, 750–760.
32 U. Hossain, A. K. Das, S. Ghosh and P. C. Sil, *Food Chem. Toxicol. Int. J. Publ. Br. Ind. Biol. Res. Assoc.*, 2020, **145**, 111738.
33 L. Qi, T. Shuai, J. Da, B. Ezra and S.-D. Luis, *Bio-Protoc.*, 2020, **10**, e3717.
34 Y. Yao, L. Yan, H. Chen, N. Wu, W. Wang and D. Wang, *Phytomedicine Int. J. Phytother. Phytopharm.*, 2020, **77**, 153268.
35 I. Hwang, Y. J. Park, Y.-R. Kim, Y. N. Kim, S. Ka, H. Y. Lee, J. K. Seong, Y.-J. Seok and J. B. Kim, *FASEB J. Off. Publ. Fed. Am. Soc. Exp. Biol.*, 2015, **29**, 2397–2411.
36 J. E. Ayala, D. P. Bracy, T. Hansotia, G. Flock, Y. Seino, D. H. Wasserman and D. J. Drucker, *Diabetes*, 2008, **57**, 288–297.
37 Y. Wang, D. Dilidaxi, Y. Wu, J. Sailike, X. Sun and X.-H. Nabi, *Biomed. Pharmacother.*, 2020, **125**, 109914.